

## Supporting Information

### **Graphene oxide–molecular Cu porphyrin integrated BiVO<sub>4</sub> photoanode for improved photoelectrochemical water oxidation performance**

Chunjiang Xu,<sup>‡a</sup> Wanjun Sun,<sup>‡a</sup> Yinjuan Dong,<sup>a</sup> Congzhao Dong,<sup>a</sup> Qiyu Hu,<sup>a</sup>  
Baochun Ma,<sup>a</sup> Yong Ding<sup>\*ab</sup>

<sup>a</sup> State Key Laboratory of Applied Organic Chemistry, Key Laboratory of Nonferrous Metals Chemistry and Resources Utilization of Gansu Province, and College of Chemistry and Chemical Engineering, Lanzhou University, Lanzhou 730000, China

<sup>b</sup> State Key Laboratory for Oxo Synthesis and Selective Oxidation, Lanzhou Institute of Chemical Physics, Chinese Academy of Sciences, Lanzhou 730000, China

<sup>‡</sup> These authors contributed equally to this work.

E-mail: dingyong1@lzu.edu.cn.

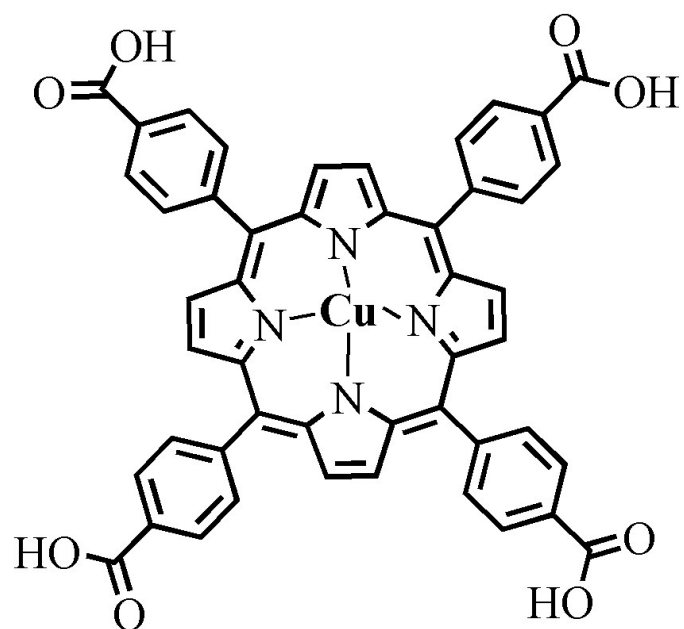


Figure S1. Structure of molecular Cu porphyrin (CuTCPP).

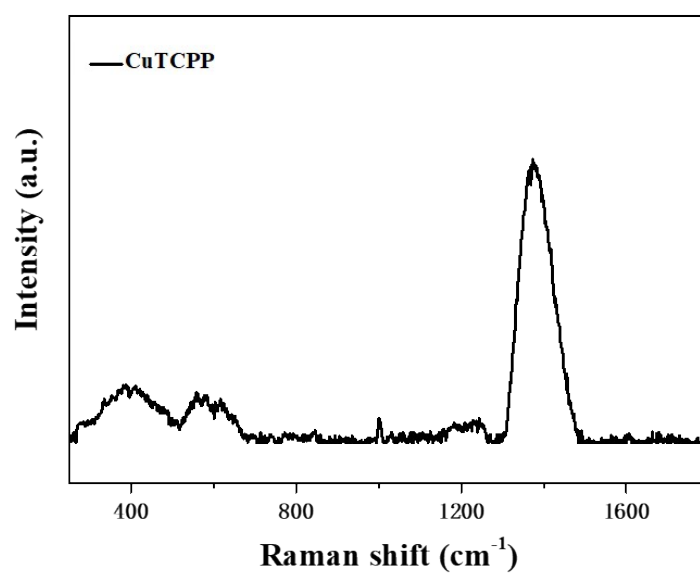


Figure S2. Raman spectrum of CuTCPP powder.

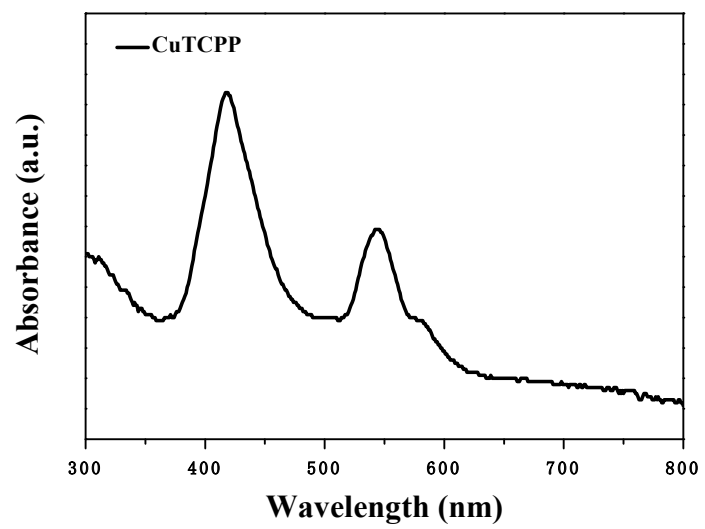


Figure S3. UV-vis diffuse reflectance spectrum of CuTCPP powder.

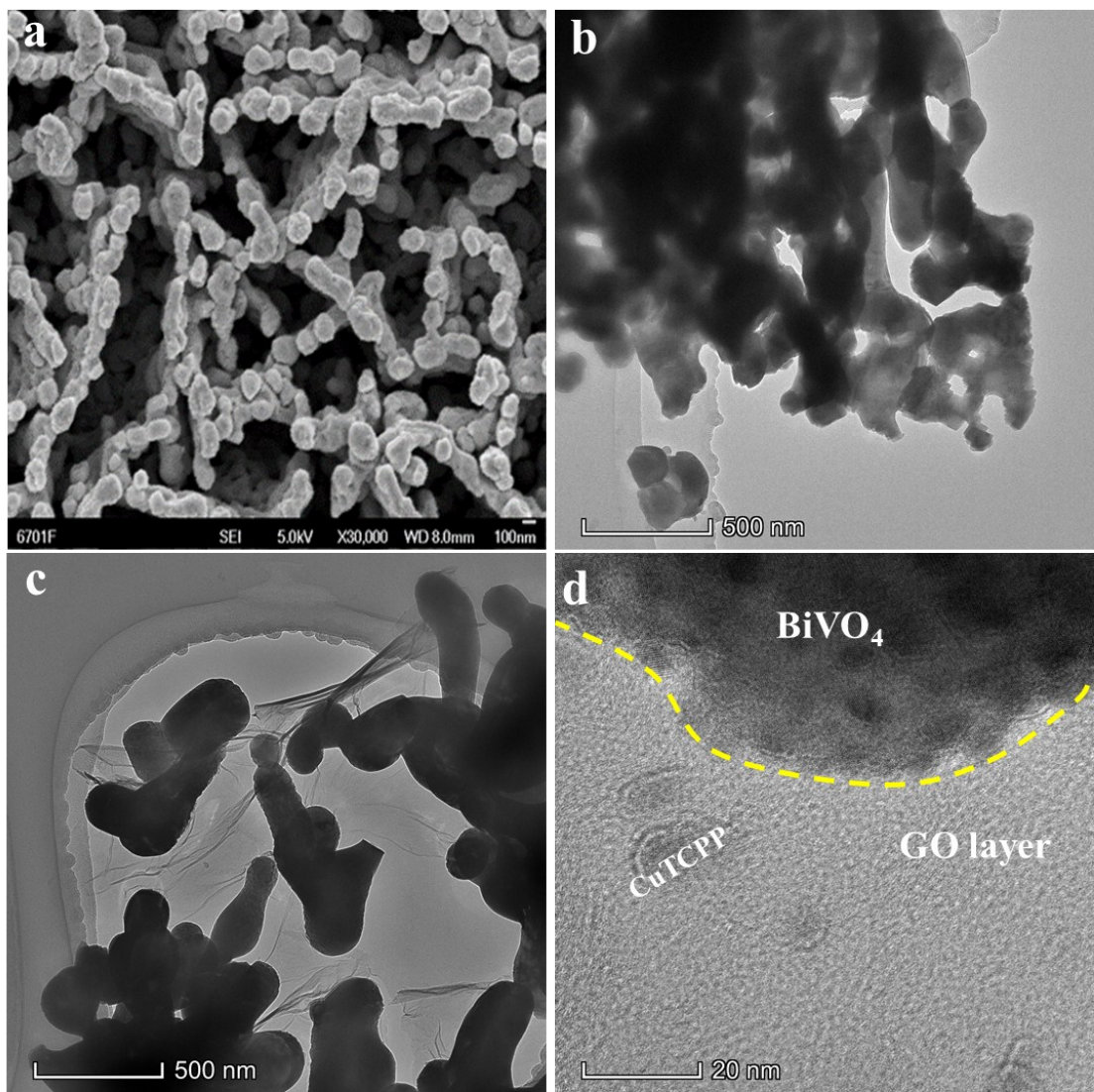


Figure S4. SEM image of (a) bare  $\text{BiVO}_4$  electrode and TEM images of (b) bare  $\text{BiVO}_4$  electrode, (c)  $\text{GO}/\text{BiVO}_4$  electrode, (d) HRTEM of  $\text{CuTCPP}/\text{GO}/\text{BiVO}_4$  electrode after reaction.

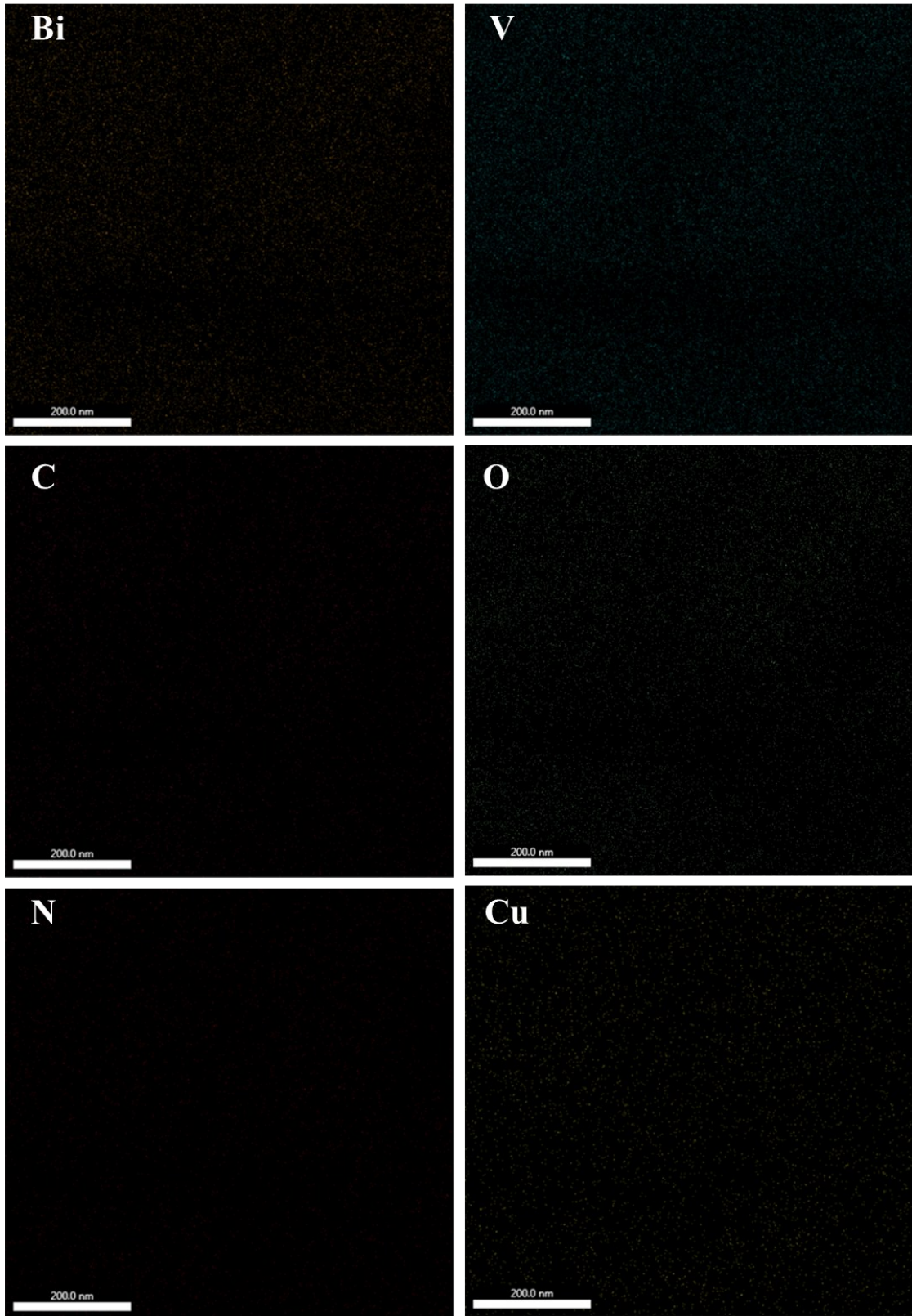


Figure S5. EDS mapping images of CuTCPP/GO/BiVO<sub>4</sub> electrode.

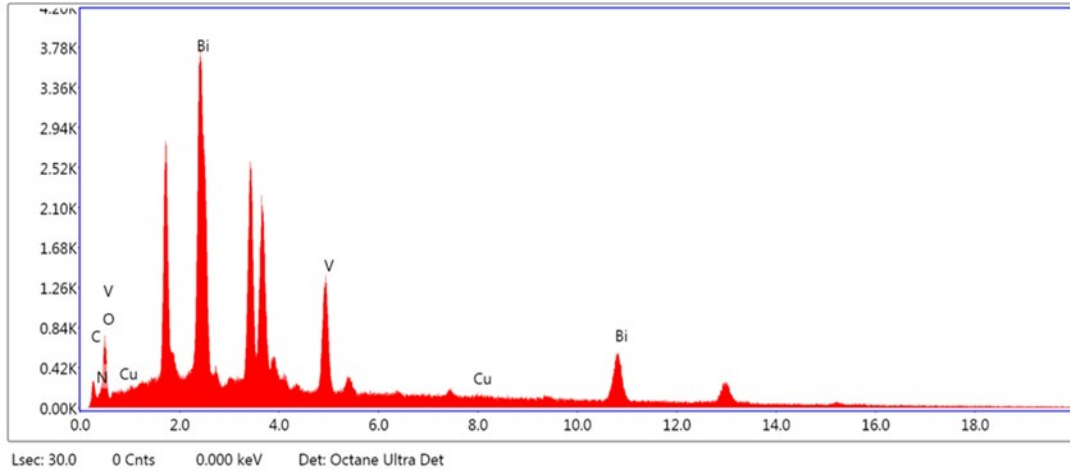


Figure S6. EDS element distribution of CuTCPP/GO/BiVO<sub>4</sub> photoanode.

Table S1. EDS analysis data of CuTCPP/GO/BiVO<sub>4</sub> photoanode.

Element <sup>↵</sup>	Weight % <sup>↵</sup>	Atomic % <sup>↵</sup>	Net Int. <sup>↵</sup>	Error % <sup>↵</sup>	Kratio <sup>↵</sup>	Z <sup>↵</sup>	R <sup>↵</sup>	A <sup>↵</sup>	F <sup>↵</sup>
C K <sup>↵</sup>	9.87 <sup>↵</sup>	27.28 <sup>↵</sup>	65.02 <sup>↵</sup>	9.53 <sup>↵</sup>	0.0579 <sup>↵</sup>	1.2760 <sup>↵</sup>	0.7973 <sup>↵</sup>	0.4601 <sup>↵</sup>	1.0000 <sup>↵</sup>
N K <sup>↵</sup>	4.49 <sup>↵</sup>	10.64 <sup>↵</sup>	14.29 <sup>↵</sup>	24.68 <sup>↵</sup>	0.0107 <sup>↵</sup>	1.2551 <sup>↵</sup>	0.8092 <sup>↵</sup>	0.1901 <sup>↵</sup>	1.0000 <sup>↵</sup>
O K <sup>↵</sup>	21.67 <sup>↵</sup>	44.98 <sup>↵</sup>	115.82 <sup>↵</sup>	13.21 <sup>↵</sup>	0.0347 <sup>↵</sup>	1.2366 <sup>↵</sup>	0.8201 <sup>↵</sup>	0.1294 <sup>↵</sup>	1.0000 <sup>↵</sup>
V K <sup>↵</sup>	13.46 <sup>↵</sup>	8.77 <sup>↵</sup>	535.36 <sup>↵</sup>	5.01 <sup>↵</sup>	0.1093 <sup>↵</sup>	0.9944 <sup>↵</sup>	0.9470 <sup>↵</sup>	0.7646 <sup>↵</sup>	1.0679 <sup>↵</sup>
Cu K <sup>↵</sup>	0.81 <sup>↵</sup>	0.43 <sup>↵</sup>	26.38 <sup>↵</sup>	34.33 <sup>↵</sup>	0.0097 <sup>↵</sup>	0.9849 <sup>↵</sup>	0.9854 <sup>↵</sup>	0.9201 <sup>↵</sup>	1.3155 <sup>↵</sup>
Bi L <sup>↵</sup>	49.71 <sup>↵</sup>	7.90 <sup>↵</sup>	349.02 <sup>↵</sup>	9.35 <sup>↵</sup>	0.4475 <sup>↵</sup>	0.7578 <sup>↵</sup>	1.1735 <sup>↵</sup>	1.0352 <sup>↵</sup>	1.1476 <sup>↵</sup>

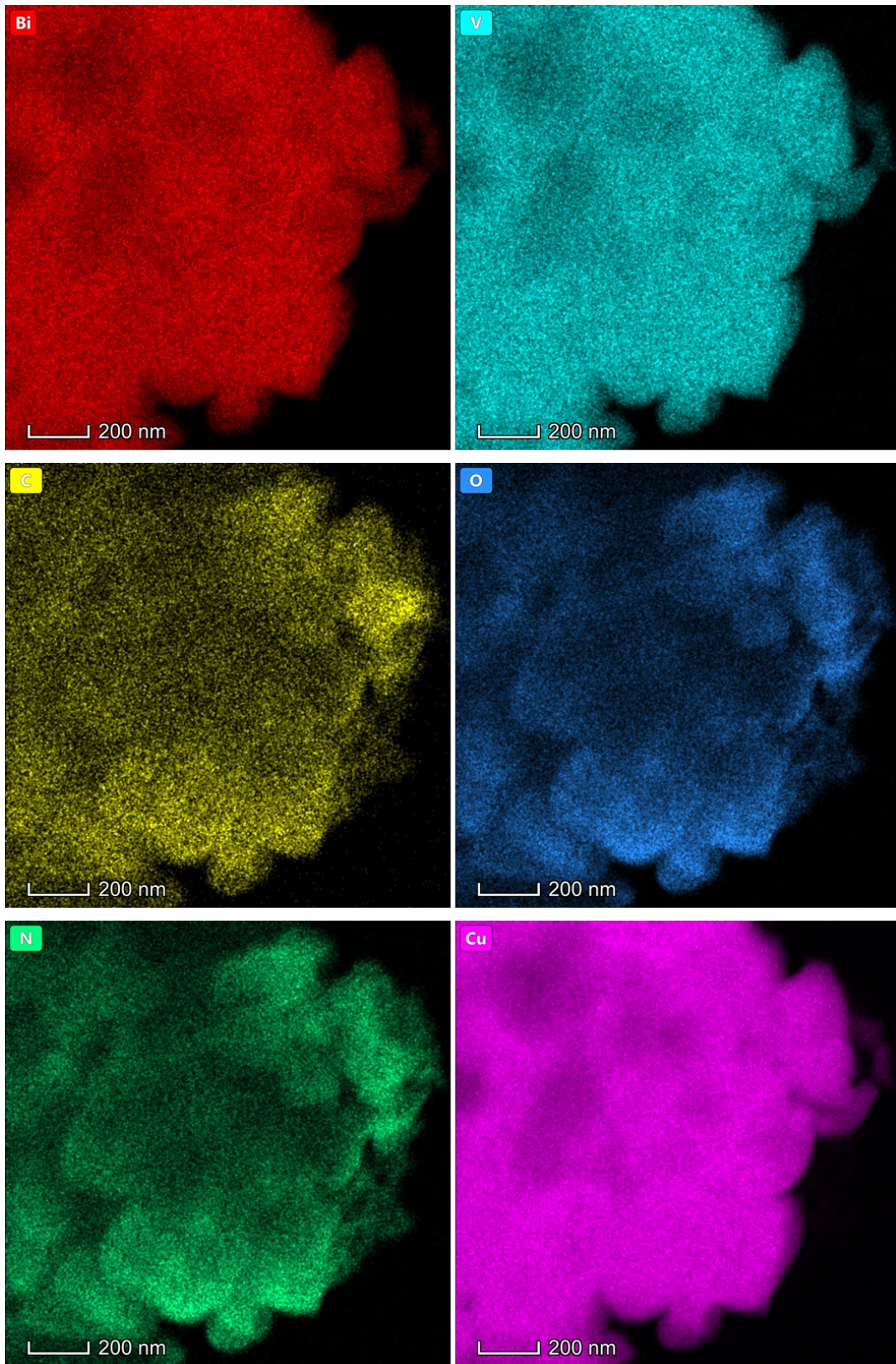


Figure S7. Elements mapping of CuTCPP/GO/BiVO<sub>4</sub> photoanode.

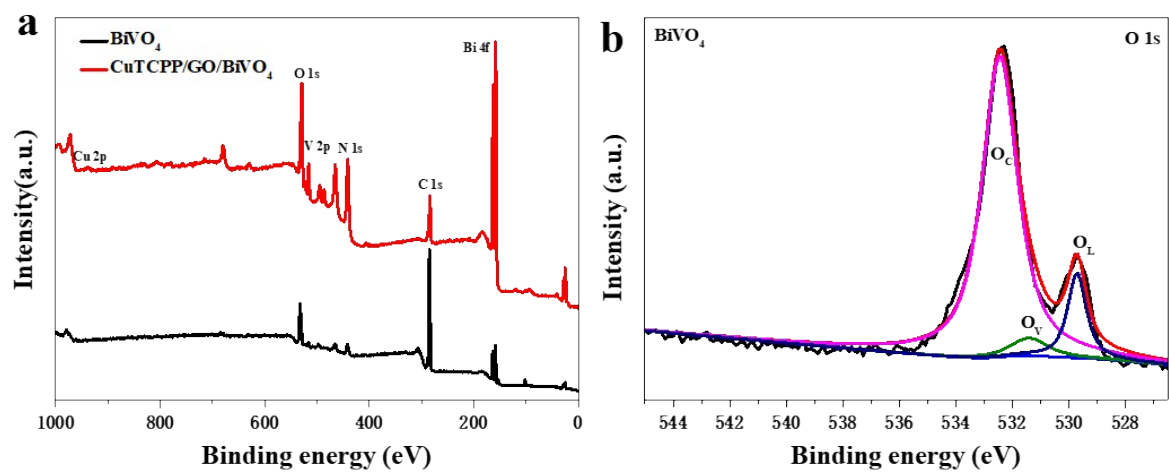


Figure S8. XPS of  $\text{BiVO}_4$  and the  $\text{CuTCPP/GO/BiVO}_4$  photoanodes a) survey and b) XPS high-resolution spectra of O 1s of  $\text{BiVO}_4$ .



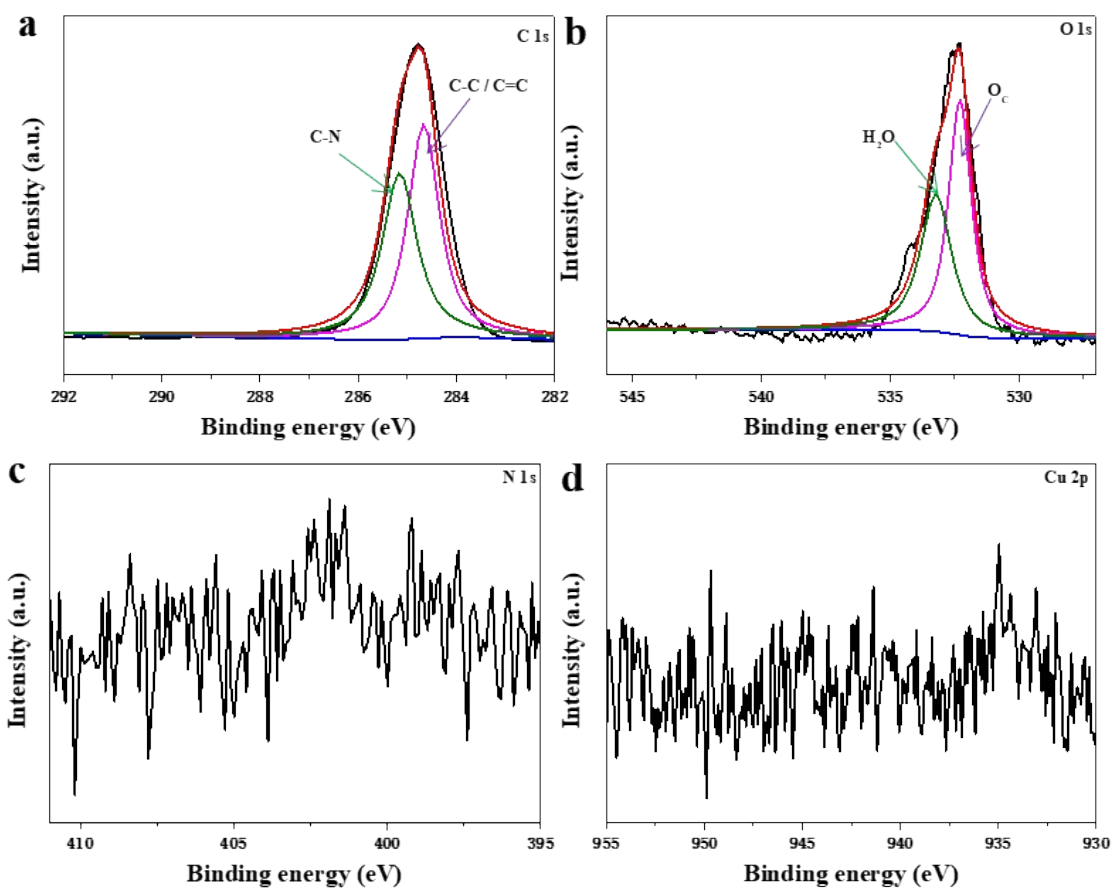


Figure S9. XPS high-resolution spectra of CuTCPP powder: a) C 1s, b) O 1s, c) N 1s and d) Cu 2p.

The water ( $\sim 533.4\text{eV}$ ) and O<sub>C</sub> ( $\sim 532.5\text{ eV}$ ) peaks of the XPS O 1s spectra of CuTCPP could be evidently detected [1,2].

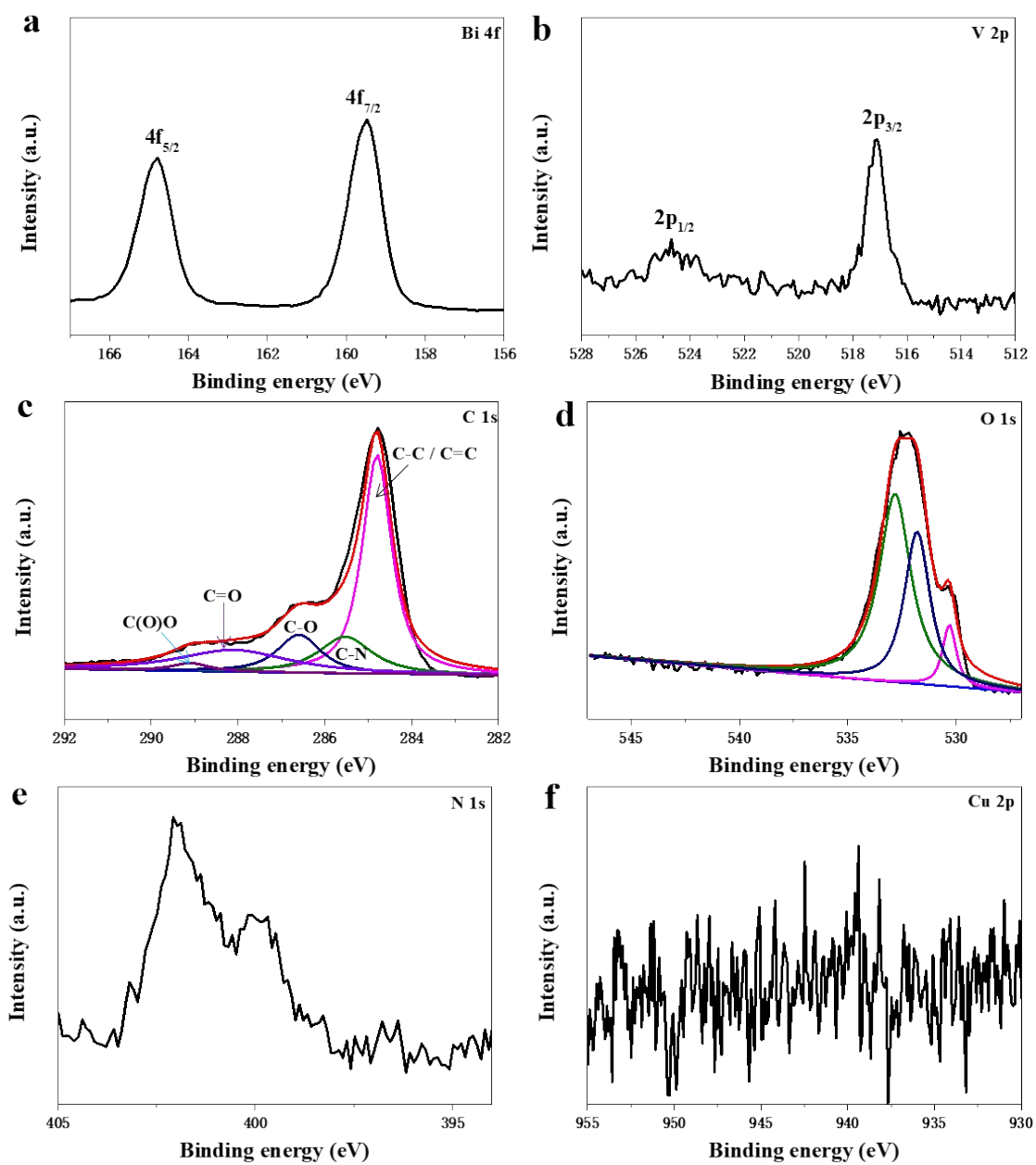


Figure S10. XPS spectra of the CuTCPP/GO/BiVO<sub>4</sub> photoanode after reaction: a) Bi 4f, b) V 2p, c) C 1s, d) O 1s, e) N 1s, and f) Cu 2p;

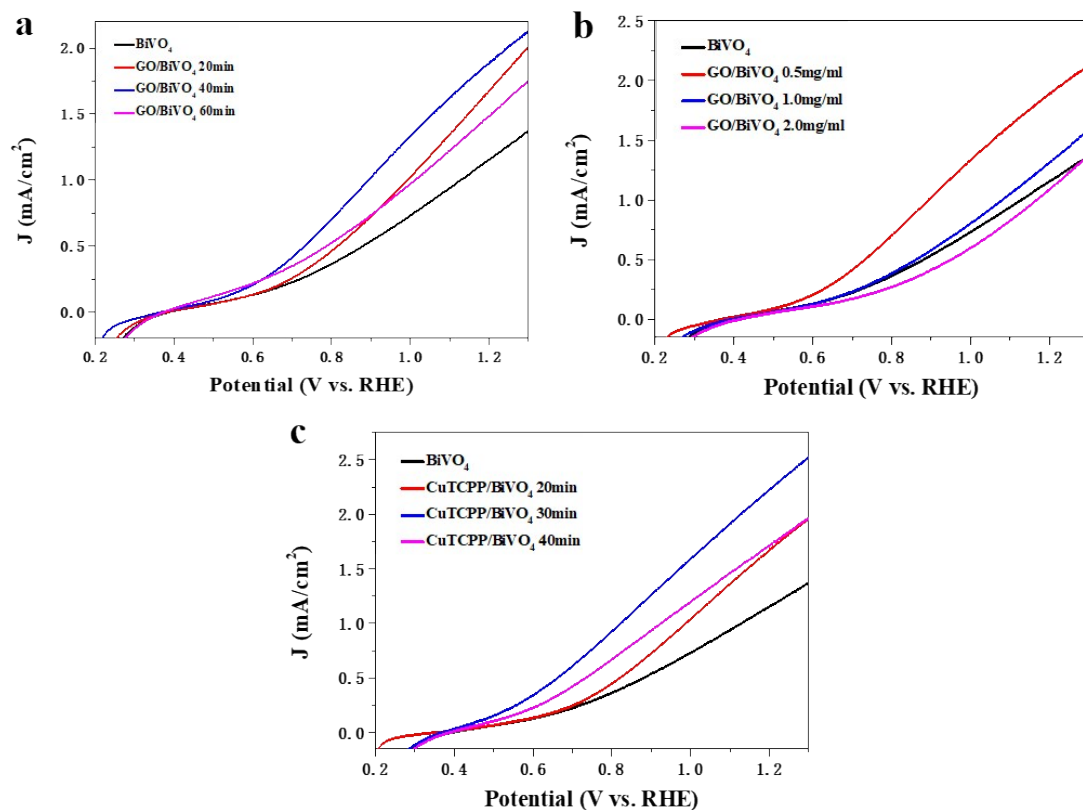


Figure S11. The LSV curves of (a) BiVO<sub>4</sub> photoanodes were treated different time by 0.5 mg/mL GO dispersion solution, (b) BiVO<sub>4</sub> photoanodes were treated different concentration of GO dispersion solution, and (c) BiVO<sub>4</sub> photoanodes were treated different time with CuTCPP dispersion solution.

As shown in Figure S11a, it indicates that BiVO<sub>4</sub> was treated by 0.5 mg mL<sup>-1</sup> GO dispersion solution with 40 min, which the photocurrent density achieves about 1.96 mA cm<sup>-2</sup> at 1.23 V vs. RHE. BiVO<sub>4</sub> photoanode was treated by CuTCPP dispersion solution with 30 min, which the photocurrent density reaches 2.2 mA cm<sup>-2</sup> at 1.23 V vs. RHE (Figure S11c).

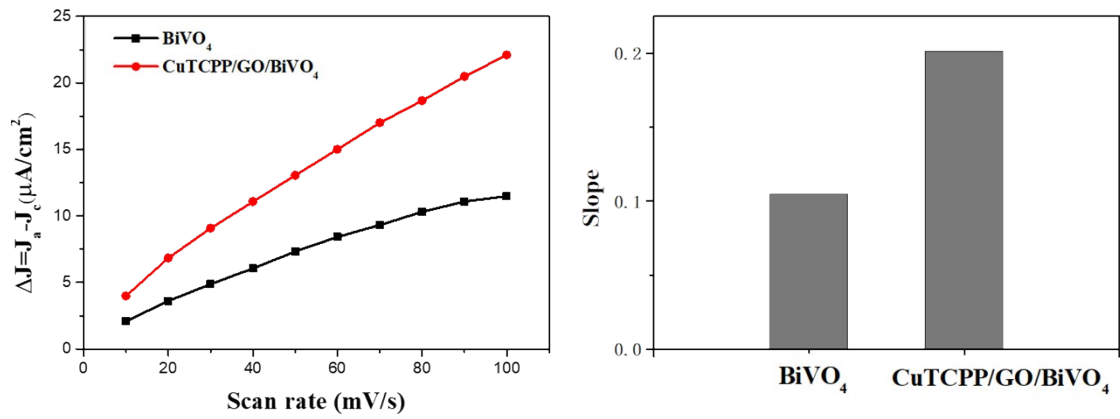


Figure S12. (a) Charging current density differences of bare  $\text{BiVO}_4$  and  $\text{CuTCPP}/\text{GO}/\text{BiVO}_4$  plotted against scan rates. (b) Slopes calculated from the fitting results of bare  $\text{BiVO}_4$  and  $\text{CuTCPP}/\text{GO}/\text{BiVO}_4$ .

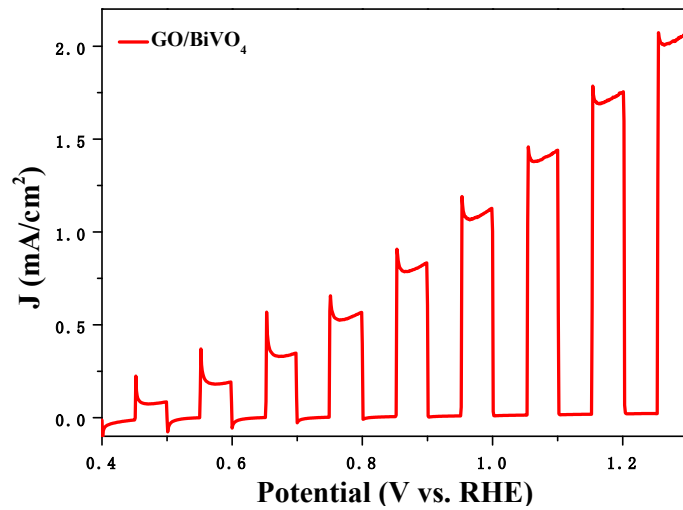


Figure S13. LSV chopping of  $\text{GO}/\text{BiVO}_4$  photoanode.

Evident transient anodic peaks are observed under dark/light, illustrating that photogenerated holes are collected in the GO layer [3,4].

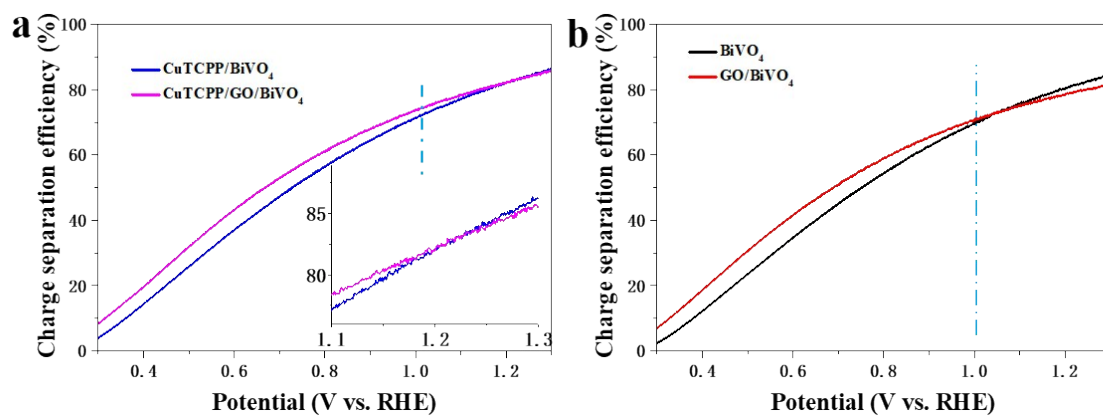


Figure S14. a) Charge separation efficiency of CuTCPP/BiVO<sub>4</sub> and CuTCPP/GO/BiVO<sub>4</sub>, b) Charge separation efficiency of GO/BiVO<sub>4</sub> and BiVO<sub>4</sub>.

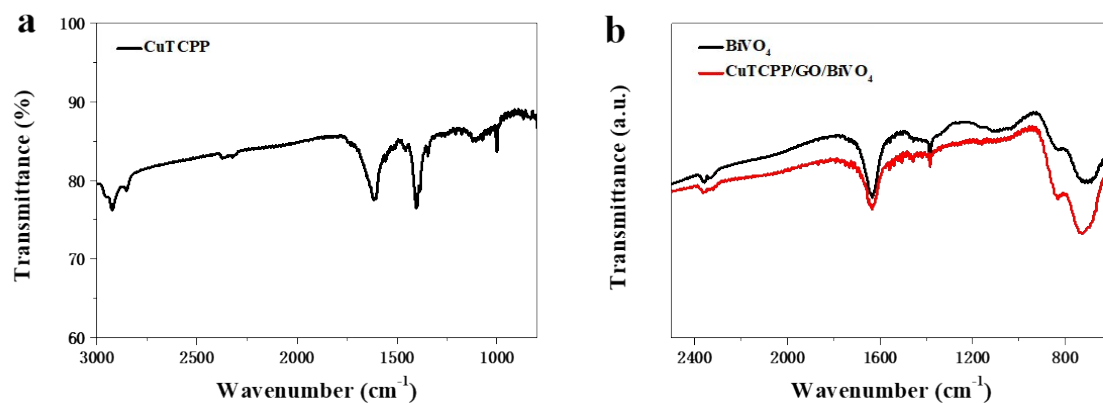


Figure S15. (a) IR spectrum of CuTCPP powder, (b) IR spectroscopy of bare BiVO<sub>4</sub> and CuTCPP/GO/BiVO<sub>4</sub> electrodes.

## Reference

1. Y. Zhang, J. Liu, Y. Zhang and Y. Bi, *Nano Energy*, 2018, **51**, 504-512.
2. Y. Zhang, Z. Xu, G. Li, X. Huang, W. Hao and Y. Bi, *Angew. Chem., Int. Ed.*, 2019, **58**, 14229-14233.
3. M. J. Bröcker, J. M. L. Ho, G. M. Church, D. Söll and P. O'Donoghue, *Angew. Chem., Int. Ed.*, 2014, **53**, 11926-11930.
4. S. Ye, C. Ding, R. Chen, F. Fan, P. Fu, H. Yin, X. Wang, Z. Wang, P. Du and Can. Li, *J. Am. Chem. Soc.*, 2018, **140**, 3250-3256.